The Astrophysical Journal Letters, 917:L9 (7pp), 2021 August 10 https://doi.org/10.3847/2041-8213/ac15f6
© 2021. The American Astronomical Society. All rights reserved.

Compact Elliptical Galaxies Hosting Active Galactic Nuclei in Isolated Environments

Soo-Chang Rey[1], Kyuseok Oh[2], and Suk Kim[1]
[1] Department of Astronomy and Space Science, Chungnam National University, Daejeon 34134, Republic of Korea; screy@cnu.ac.kr
[2] Korea Astronomy and Space Science Institute, Daedeokdae-ro 776, Yuseong-gu, Daejeon 34055, Republic of Korea; oh@kasi.re.kr
Received 2021 April 28; revised 2021 July 12; accepted 2021 July 20; published 2021 August 12

Abstract

We present the discovery of rare active galactic nuclei (AGNs) in nearby ($z < 0.05$) compact elliptical galaxies (cEs) located in isolated environments. Using spectroscopic data from the Sloan Digital Sky Survey (SDSS) Data Release 12, four AGNs were identified based on the optical emission-line diagnostic diagram. SDSS optical spectra of AGNs show the presence of distinct narrow-line emissions. Utilizing the black hole (BH) mass–stellar velocity dispersion scaling relation and the correlation between the narrow $L([\mathrm{O\,III}])/L(\mathrm{H}\beta)$ line ratio and the width of the broad Hα emission line, we estimated the BH masses of the cEs to be in the range of 7×10^5–$8 \times 10^7\,M_\odot$. The observed surface brightness profiles of the cEs were fitted with a double Sérsic function using the Dark Energy Camera Legacy Survey *r*-band imaging data. Assuming the inner component as the bulge, the *K*-band bulge luminosity was also estimated from the corresponding Two Micron All Sky Survey images. We found that our cEs follow the observed BH mass–stellar velocity dispersion and BH mass–bulge luminosity scaling relations, albeit there was a large uncertainty in the derived BH mass of one cE. In view of the observational properties of BHs and those of the stellar populations of cEs, we discuss the proposition that cEs in isolated environments are bona fide low-mass early-type galaxies (i.e., a nature origin).

Unified Astronomy Thesaurus concepts: Elliptical galaxies (456); Black holes (162); Active galactic nuclei (16); Compact galaxies (285); Galaxy formation (595); Galaxy evolution (594)

1. Introduction

In the nearby universe, compact elliptical galaxies (cEs) are a rare class of non-star-forming objects that are typically characterized by compact sizes (100–900 pc), low stellar masses (10^8–$10^{10}\,M_\odot$), and very high stellar densities. Only a few hundred cEs are currently known (Chilingarian et al. 2009; Norris et al. 2014; Chilingarian & Zolotukhin 2015; Kim et al. 2020). They conform to the low-mass regime of the mass–size relation defined by massive early-type galaxies. Although the origin of cEs is still a subject of debate (Bekki et al. 2001; Martinović & Micic 2017; Du et al. 2019; Urrutia Zapata et al. 2019), cEs are thought to be a mixture of objects formed via two main channels (i.e., nature or nurture) depending on their local environment (i.e., without or with a nearby massive host galaxy; Ferré-Mateu et al. 2018, 2021a; Kim et al. 2020).

The prevailing scenario is that progenitors of cEs are larger, more massive galaxies, and their outer envelopes are stripped by dissipative tidal interactions with a more massive neighboring host galaxy. In this process, cEs are the tidally stripped central remnants of their massive progenitors (i.e., stripped cEs). This scenario is supported by the fact that a large fraction of cEs are associated with an adjacent massive host galaxy (Norris et al. 2014; Chilingarian & Zolotukhin 2015; Janz et al. 2016; Kim et al. 2020). In addition, the metallicities of most cEs with a massive host galaxy are higher than those of low-mass galaxies with similar masses, but are comparable to those of more massive galaxies (e.g., Kim et al. 2020). The discovery of tidal streams around a few cEs that are being stripping by their host galaxy provides further direct evidence for this scenario (e.g., Huxor et al. 2011; Paudel & Ree 2014; Ferré-Mateu et al. 2018).

However, the discovery of some isolated cEs with no neighboring massive host galaxy suggests an additional origin of cEs (Huxor et al. 2013; Paudel et al. 2014). Such cEs are intrinsically low-mass, compact galaxies formed at very early cosmic times without acquiring ex situ stellar mass in their evolutionary histories (i.e., intrinsic cEs). In this case, they represent the low-luminosity extension of luminous elliptical galaxies, which is supported by the fact that cEs follow the scaling relations of classical elliptical galaxies (e.g., Wirth & Gallagher 1984; Kormendy et al. 2009; Kormendy & Bender 2012). For example, most isolated cEs follow the mass–metallicity relation of massive early-type galaxies at the low-mass regime (e.g., Kim et al. 2020).

There is a correlation between the masses of black holes (BHs) and bulge masses of the galaxies that host them (e.g., Kormendy & Ho 2013). In this regard, predictions for different BH masses of cEs are expected, depending on the formation channel. If cEs are formed through a stripping process, they might host supermassive BHs appropriate for their massive progenitors. In contrast, if cEs are low-mass versions of classical early-type galaxies, they will instead host intermediate BHs in accordance with their low stellar masses. Moreover, the incidence of active galactic nucleus (AGN) activity also provides an important constraint on the star formation history and environment of cEs, which are closely related to the gas reservoir that can trigger the nuclear activity within galaxies (Aird et al. 2019; Man et al. 2019, and references therein). Thus, the BH properties of cEs would further provide independent tracers for probing the origins of cEs.

However, observational hints of the existence of BHs in cEs have been reported for only a handful to date (e.g., Kormendy et al. 1997; van der Marel et al. 1997; Mieske et al. 2013; Paudel et al. 2016). Moreover, a direct optical signature of an accreting BH has been discovered for only one cE using the Sloan Digital Sky Survey (SDSS) spectra (Paudel et al. 2016). In this work, based on our large sample of cEs (Kim et al. 2020), we report the discovery of rare cEs that exhibit AGN activity possessing narrow-line emissions in their SDSS optical spectra. The remainder of this Letter is organized as follows. In Section 2, we describe the identification of cEs with AGNs (hereafter $\mathrm{cE_{AGNs}}$) and their structural properties. In Section 3,

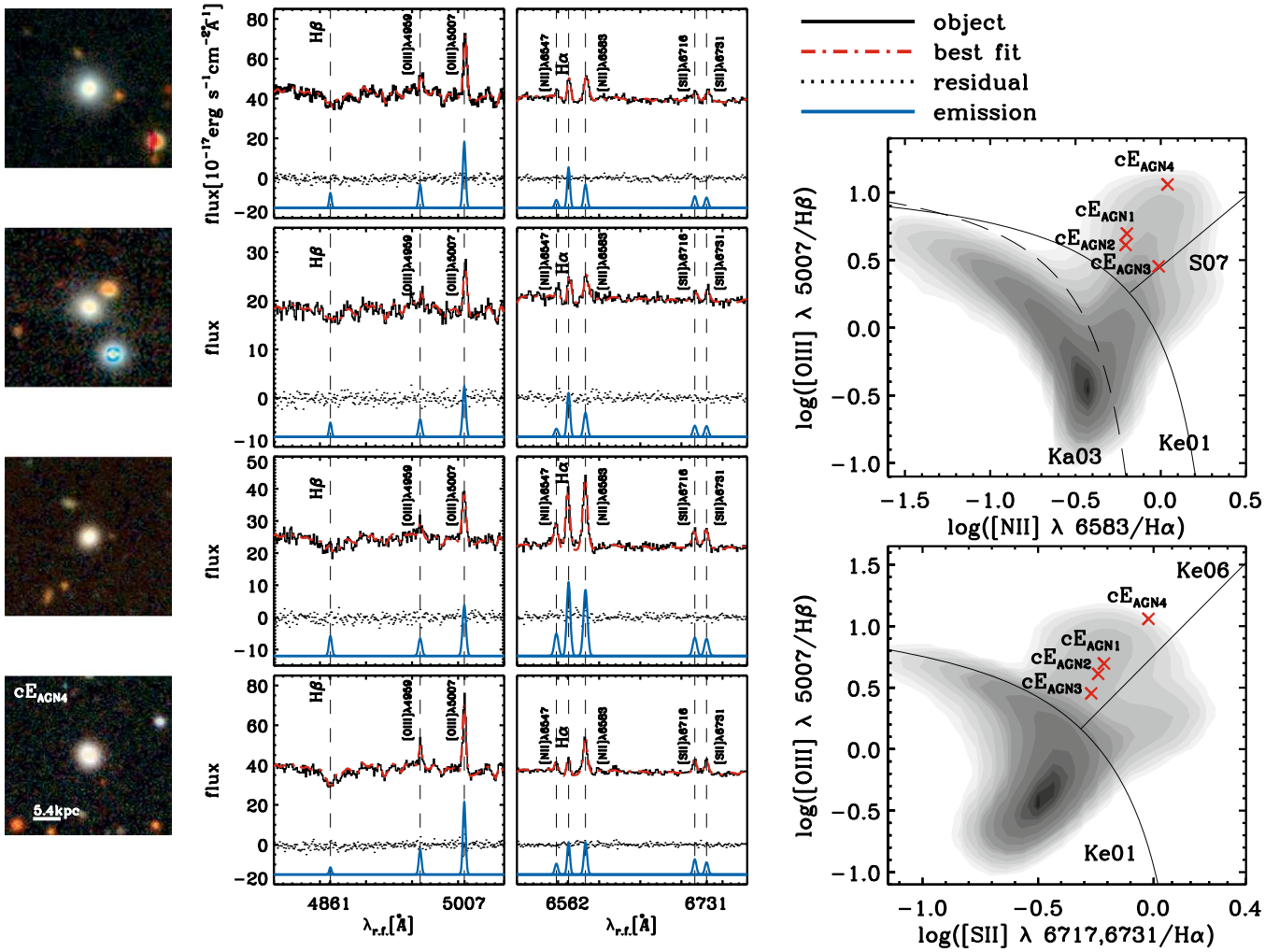


Figure 1. Left: Dark Energy Camera Legacy Survey (DECaLS) g, r, and z composite color images of the four cE$_{AGNs}$. Middle: observed spectrum (black), the best fit (red dotted–dashed), residuals (black dots), and detected emission lines (blue) of the cE$_{AGNs}$. Right: BPT diagnostic diagrams. The cE$_{AGNs}$ (red crosses) and emission-line galaxies with amplitude-over-noise ratio (A/N) cut (>3 for [N II]λ6583, Hα, [O III]λ5007, Hβ, and [S II]λ6717, 6731; $N \approx 180{,}000$) chosen from the entire OSSY catalog at $z < 0.2$ (filled contours; Oh et al. 2011) are shown.

we present the environment of these cE$_{AGNs}$ and derive estimations of their BH masses. In Section 4, we discuss a possible formation scenario for cE$_{AGNs}$ in isolated environments. Throughout this study, we assume the cosmological parameters to be $\Omega_m = 0.3$, $\Omega_\Lambda = 0.7$, and $h_0 = 0.73$.

2. Sample and Analysis

We have recently constructed a new catalog of cEs in the local volume ($z < 0.05$) using the SDSS DR12 (Kim et al. 2020). Following the conventional selection criteria of cEs, 138 cEs with sizes smaller than 600 pc were selected for the final sample (see Kim et al. 2020, for more details on the selection of cEs). Kim et al. (2020) also investigated the stellar population properties (i.e., age and [Z/H]) of cEs based on the Lick indices obtained from the SDSS spectra by comparing them to simple stellar population model grids.

2.1. Identifying AGNs

We performed spectral line fitting for the 138 cEs using the `gandalf` (Sarzi et al. 2006), which was later modified to measure nebular emission lines, stellar absorption lines, and stellar velocity dispersions for more than 660,000 SDSS galaxies at $z < 0.2$ (Oh et al. 2011, 2015).

Our analysis of the cE SDSS spectra consisted of three major steps. First, we deredshifted the spectra and corrected the effect of Galactic foreground extinction (Schlafly & Finkbeiner 2011). Second, we extracted the stellar kinematics by matching the spectra with a set of stellar templates. The spectral regions that were potentially affected by nebular emission lines were masked in this process. We employed the Penalized PiXel-Fitting method (`pPXF`; Cappellari & Emsellem 2004) using the synthesized stellar population models (Bruzual & Charlot 2003) and the MILES empirical stellar libraries (Sánchez-Blázquez et al. 2006). Finally, we simultaneously measured the strength of the emission lines using both the stellar templates that were derived in the previous step and a set of Gaussian templates that represent the emission lines. In this process, we combined the stellar templates with a number of Gaussian emission line templates described either by single Gaussians or by sets of Gaussians that characterize doublets (e.g., the middle panels in Figure 1).

Using the measured emission line ratios ([N II]λ6583/Hα, [O III]λ5007/Hβ, and [S II]λ6717, 6731/Hα), we identified four type 2 (obscured) AGNs that possess optical spectral

energy distributions dominated by stellar continua, but also narrow emission line ratios falling into the Seyfert regime in the BPT diagram (Baldwin et al. 1981, see right panels in Figure 1). For the latter, we used the theoretical maximum starburst model (Kewley et al. 2001) and the empirical star formation curve (Kauffmann et al. 2003). Additionally, in order to discriminate low-ionization nuclear emission line regions from Seyfert AGNs, we used the demarcation lines derived by Schawinski et al. (2007) and Kewley et al. (2006). A Gaussian amplitude-over-noise ratio (A/N) greater than 3 was used for the emission lines ([N II]λ6583, Hα, [O III]λ5007, Hβ, and [S II]λ6717, 6731). Moreover, the four cE$_{\rm AGNs}$ of this study have been also identified by Ferré-Mateu et al. (2021b).

2.2. Structural Parameters

We used the Dark Energy Camera Legacy Survey (DECaLS) imaging data to derive the structural parameters of the four cE$_{\rm AGNs}$. With an average seeing of $1\farcs18$ and a pixel scale of 0.262 arcsec/pix (Dey et al. 2019), the DECaLS r-band imaging of the cE$_{\rm AGNs}$ provide better quality data than the SDSS images (see Figure 1). All of the objects in each DECaLS image detected by SExtractor (Bertin & Arnouts 1996), except the cE$_{\rm AGN}$ itself, were removed by replacing their flux with the median background flux calculated from all the surrounding pixels in the image.

We determined the surface brightness profiles of the cE$_{\rm AGNs}$ using the IRAF *ellipse* task, fitting them with a single Sérsic function and a double Sérsic function. In the case of the double Sérsic function, we fixed the outer component as an exponential profile with a Sérsic index of n = 1. Based on the residuals between the observed surface brightness profiles and their model fits, we found that all four cE$_{\rm AGNs}$ are better fitted by a double Sérsic function with Sérsic indices for the inner component in the range of 0.8–1.1. We also derived the near-infrared K-band total luminosity enclosed within a Petrosian aperture by using SExtractor to obtain the photometry in the 2MASS archival images. Assuming the inner component as the bulge, the K-band bulge luminosity was calculated using the flux ratio between the inner and outer components (Paudel et al. 2016). The basic properties of the four cE$_{\rm AGNs}$ are listed in Table 1.

3. Results

3.1. Environment

In our previous work, we defined the environment of our 138 cE sample (see Kim et al. 2020 for details). The local environment (with and without a bright host galaxy) was quantified using the projected distance from each cE to the nearest luminous ($M_r < -21.0$ mag) galaxy with a relative velocity of less than 500 km s^{-1}. If a cE is inside (or outside) the virial radius ($R_{\rm vir}$) of the nearest luminous galaxy, the cE was classified as having (or not having) a host galaxy. All cE$_{\rm AGNs}$ are located at least four times beyond the $R_{\rm vir}$ of a luminous neighbor galaxy, indicating a low likelihood of gravitational interaction with nearby galaxies. Therefore, the cE$_{\rm AGNs}$ are defined as those without an associated host galaxy. Following Norris et al. (2014), the global environment (i.e., cluster, group, and field) of the cE$_{\rm AGNs}$ was also defined using the group catalog of Tempel et al. (2014). This resulted in all the cE$_{\rm AGNs}$ being classified as field galaxies (see Kim et al. 2020). Consequently, given the local and global environments surrounding the cE$_{\rm AGNs}$, we suggest that all cE$_{\rm AGNs}$ are located in isolated environments.

3.2. BH Mass and Scaling Relations

Having measured the stellar velocity dispersions (σ_*), the central BH masses ($M_{\rm BH}$) of the four cE$_{\rm AGNs}$ were estimated to be in the range of $(3.1–9.8) \times 10^6$ $M_\odot$ using the $M_{\rm BH} - \sigma_*$ relation from Kormendy & Ho (2013). Based on the spectral resolution of SDSS, a reliable estimate for σ_* is known as $\sigma_* > 60$ km s^{-1}. If the scaling relation from Gültekin et al. (2009) is adopted, we obtained approximately 0.3 dex lower for the $M_{\rm BH}$.

Because a single epoch method is not applicable for our cE$_{\rm AGNs}$ owing to a lack of broad lines[3], we attempted to estimate $M_{\rm BH}$ independently using the relation between the narrow L([O III])/L(Hβ) line ratio and the width of the broad Hα emission line (FWHM$_{\rm broad\ H\alpha}$) of Baron & Ménard (2019). By using our strength measurement of emission lines ([O III] λ5007 and Hβ), the $M_{\rm BH}$ values of the cE$_{\rm AGNs}$ were estimated to be in the range of 7×10^5–8×10^7 $M_\odot$. For comparison, we also estimated $M_{\rm BH}$ by adopting the strengths of emission lines provided by Chilingarian et al. (2017), which are approximately 0.3 dex lower. It should be mentioned that the observed relationship between the L([O III])/L(Hβ) and FWHM$_{\rm broad\ H\alpha}$ of Baron & Ménard (2019) exhibits a significant scatter in the bulk population of AGNs. As a result, regardless which line strength measurements are used, the derived $M_{\rm BH}$ of cE$_{\rm AGN4}$ is high and has a large uncertainty. The estimated $M_{\rm BH}$ of the four cE$_{\rm AGNs}$ and its measurement errors are listed in Table 1. The systematic uncertainties of $M_{\rm BH}$-σ_* relation and the method of Baron & Ménard (2019) are known as 0.29 dex (Kormendy & Ho 2013) and at least 0.5 dex (Baron & Ménard 2019), respectively.

In Figure 2, we present the scaling relations between the $M_{\rm BH}$ and the properties of the cE$_{\rm AGNs}$ along with galaxies compiled from the literature. The correlations between $M_{\rm BH}$ and the stellar velocity dispersions of the galaxies (left panel) and the K-band absolute magnitudes of the galaxy bulges (right panel) are shown. The cE previously identified in isolation (blue filled square; J085431.18+173730.5, Paudel et al. 2016) and two tidally stripped cEs (M32 and NGC 4486B) that are known to contain BHs, are also presented in both panels. Overall, our cE$_{\rm AGNs}$ almost overlap with the galaxies at the low-velocity dispersion and low-luminosity ends, and are not outliers from the observed scaling relations.[4]

4. Discussion and Conclusion

4.1. Ejected Compact Ellipticals from Dense Environment?

While the isolated cEs are considered intrinsic low-mass early-type galaxies, an alternative channel for their formation has also been suggested (Chilingarian & Zolotukhin 2015). In this scenario, isolated cEs are also originally formed through tidal stripping in clusters or groups, but they are subsequently ejected from their original environments via three-body encounters.

[3] cE$_{\rm AGN3}$ may look like a broad-line AGN, but it does not pass the cut proposed by Oh et al. (2015).

[4] Note that the $M_{\rm BH}$ of the cE$_{\rm AGN4}$ derived from the method of Baron & Ménard (2019) is highly uncertain due to a significant offset of L([O III])/L(Hβ) from the bulk population of AGNs.

Table 1
Basic Properties of cEs with AGN

Galaxy	R.A.	Decl.	z	$M_{\rm r}$	$M_{\rm K,bulge}$	Age	[Z/H]	σ_*	$M_{\rm BH,\sigma}$	$M_{\rm BH,OSSY}$	$M_{\rm BH,RCSED}$	M_*
	(deg)	(deg)		(mag)	(mag)	(Gyr)		(km s^{-1})	($\log(M_\odot)$)	($\log(M_\odot)$)	($\log(M_\odot)$)	($\log(M_\odot)$)
(1)	(2)	(3)	(4)	(5)	(6)	(7)	(8)	(9)	(10)	(11)	(12)	(13)
cE$_{\rm AGN1}$(K12)	55.8761	−7.5854	0.0356	−18.87	−20.51	$2.8^{+3.0}_{-1.0}$	$-0.26^{+0.26}_{-0.27}$	85 ± 6	6.86 ± 0.22	6.59 ± 0.08	6.33 ± 0.26	9.23 ± 0.02
cE$_{\rm AGN2}$(K28)	144.3114	37.2918	0.0460	−18.65	−21.13	$2.8^{+2.8}_{-1.0}$	$-0.13^{+0.27}_{-0.20}$	91 ± 11	6.99 ± 0.27	6.22 ± 0.14	5.92 ± 0.37	9.19 ± 0.07
cE$_{\rm AGN3}$(K30)	146.2126	12.5123	0.0425	−18.62	−20.82	$3.8^{+1.6}_{-2.0}$	$-1.15^{+0.41}_{-0.38}$	70 ± 11	6.49 ± 0.34	5.87 ± 0.09	5.50 ± 0.21	9.03 ± 0.02
cE$_{\rm AGN4}$(K41)	159.8273	17.1881	0.0374	−18.94	−20.52	$1.8^{+0.8}_{-0.6}$	$-0.07^{+0.28}_{-0.26}$	75 ± 8	6.63 ± 0.27	7.91 ± 0.17	7.23 ± 0.27	9.20 ± 0.01

Note. (1) Galaxy name (the name of the Kim et al. 2020 catalog is in parenthesis); (2) R.A. (J2000) and (3) Decl. (J2000) from the SDSS; (4) redshift from the SDSS; (5) DECaLS r-band absolute magnitude from SExtractor; (6) 2MASS K-band bulge absolute magnitude measured from the SDSS spectrum; (7) age and (8) metallicity of the stellar population from Kim et al. (2020); (9) stellar velocity dispersion; (10) BH mass derived from the BH mass–stellar velocity relation of Kormendy & Ho (2013); (11) and (12) BH masses derived from the relation of Baron & Ménard (2019) using the line strength measurements of Oh et al. (2011) and Chilingarian et al. (2017), respectively; (13) stellar mass from Kim et al. (2020).

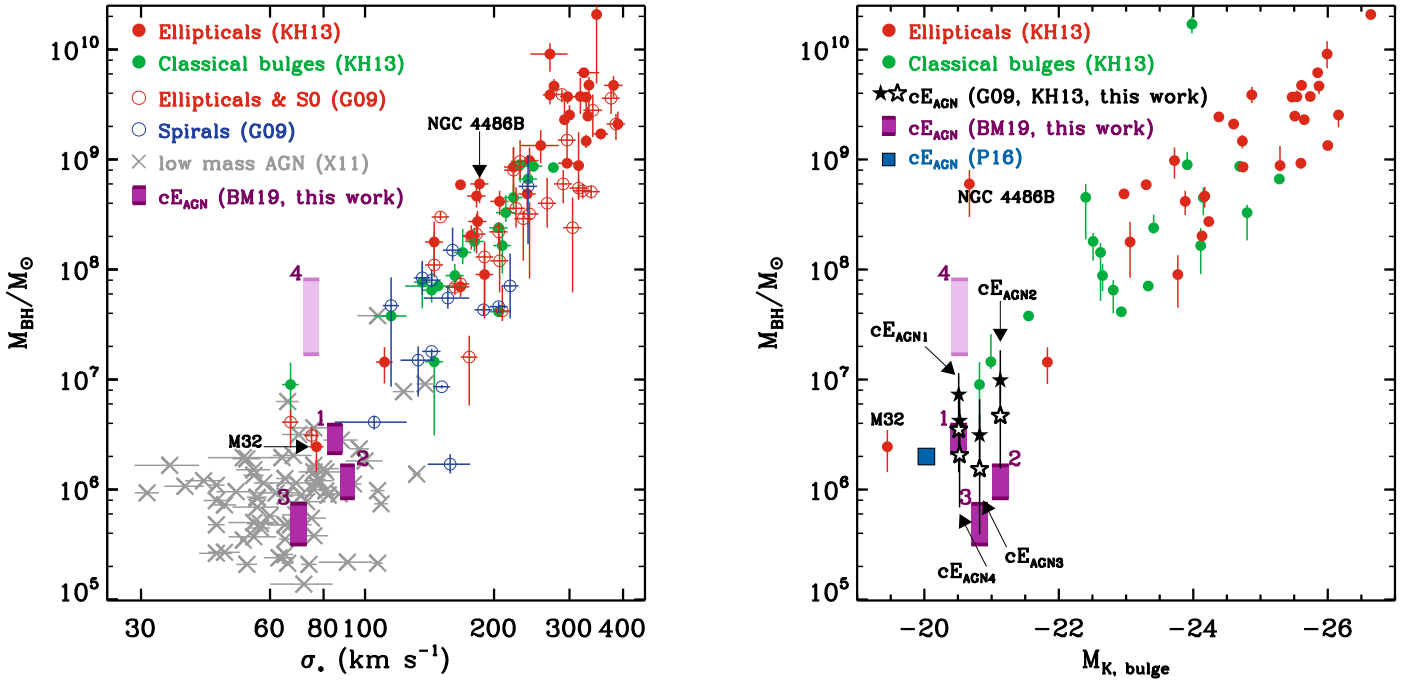


Figure 2. Left: correlation between black hole mass (M_{BH}) and stellar velocity dispersion (σ_*) of galaxies. Ellipticals (red filled circles) and classical bulges (green filled circles) from Kormendy & Ho (2013) and ellipticals/S0 (red open circles) and spirals (blue open circles) from Gültekin et al. (2009) are displayed. The gray crosses represent low-mass AGNs (Xiao et al. 2011) that do not have morphology information. Right: relation between M_{BH} and the K-band absolute magnitude for ellipticals (red filled circles) and classical bulges (green filled circles) from Kormendy & Ho (2013). The filled and open stars are the M_{BH} estimates of the cE$_{AGNs}$ following the scaling relations of Kormendy & Ho (2013) and Gültekin et al. (2009), respectively. In both panels, the M_{BH} estimates of the cE$_{AGNs}$ following Baron & Ménard (2019) are shown with purple bars. The upper and lower ends of each bar are the M_{BH} values estimated using the line strengths of Oh et al. (2011) and Chilingarian et al. (2017), respectively. The cE previously identified in isolation (blue filled square; Paudel et al. 2016) and two tidally stripped cEs (M32 and NGC 4486B) hosting BHs are shown for comparison.

Based on the group catalog of Saulder et al. (2016), for each cE$_{AGN}$ we searched for the nearest group. The ranges of the three-dimensional and sky-projected distances of three cE$_{AGNs}$ (cE$_{AGN1}$, cE$_{AGN2}$, and cE$_{AGN4}$) from their nearest groups are 4−6 Mpc and 2−6 Mpc, respectively. Considering the large physical separations, ejection from groups is improbable for these cE$_{AGNs}$. On the other hand, cE$_{AGN3}$, which is listed as a member of a very small group with only two members, is located at a distance of 5 Mpc (three-dimensional) and 0.4 Mpc (projected) from the nearest group. If the cE$_{AGN3}$ was formed through a stripping process at a very early epoch, followed by ejection from a group with a velocity comparable to the velocity dispersion of the group ($\sim$30 km s^{-1}), it would take longer than a Hubble time for the cE$_{AGN3}$ to move to its current location. Unless cE$_{AGN3}$ is an abnormal high-speed object on an extremely eccentric orbit (Sales et al. 2007; Paudel et al. 2016), we can rule out the possibility that cE$_{AGN3}$ is an object ejected from a group. Moreover, it is not possible for the ejection of a cE from its host group by three-body interaction to occur concurrently with cE formation through tidal stripping by its host galaxy (Chilingarian & Zolotukhin 2015).

In accordance with the mass–metallicity relation, if cEs with host galaxies are remnant cores of their massive progenitors that are formed through a stripping process, they would be more metal-rich than galaxies of comparably low masses (Chilingarian & Zolotukhin 2015; Janz et al. 2016; Ferré-Mateu et al. 2018, 2021a; Kim et al. 2020; see red circles for cEs with a host galaxy in Figure 3). In contrast, intrinsically low-mass cEs in isolated environments would follow the low-mass regime of the mass–metallicity relation (Kim et al. 2020; see blue circles for cEs without a host galaxy in Figure 3). If cE$_{AGNs}$ are stripped cEs, their massive progenitors would lose most of their original masses during the stripping process, but the metallicities of the central cores would remain almost unchanged. Therefore, they should deviate from the mass–metallicity relation of early-type galaxies, being more metal-rich than the metallicities expected for their stellar masses. However, as shown in Figure 3, all the cE$_{AGNs}$ appear to fall below the observed mass–metallicity distribution of cEs with a host galaxy, conforming instead to that of cEs without a host galaxy. This also supports the suggestion that all cE$_{AGNs}$ are intrinsic cEs formed in isolated environments rather than stripped cEs that were ejected from denser environments.

4.2. Origin of Isolated Compact Ellipticals: BH Perspective

The AGN fraction of galaxies is highly dependent on the environment in which AGN host galaxies reside (e.g., Man et al. 2019 and references therein); AGNs are preferentially found in lower-density environments. Galaxies in isolated environments, on average, have higher gas reservoirs for triggering AGN activity because the environmental effects required for stripping the gas are not obvious. This is in line with that our four cE$_{AGNs}$ and the previously discovered cE$_{AGN}$ with broad emission lines of an accreting BH (Paudel et al. 2016) reside in isolated environments with no nearby bright host galaxies.

Moreover, a connection between overall AGN activity and the star formations of host galaxies has been identified (Aird et al. 2019, and references therein). The availability of cold gas within galaxies may drive both AGN activity and star formation. In this respect, the stellar populations of cE$_{AGNs}$

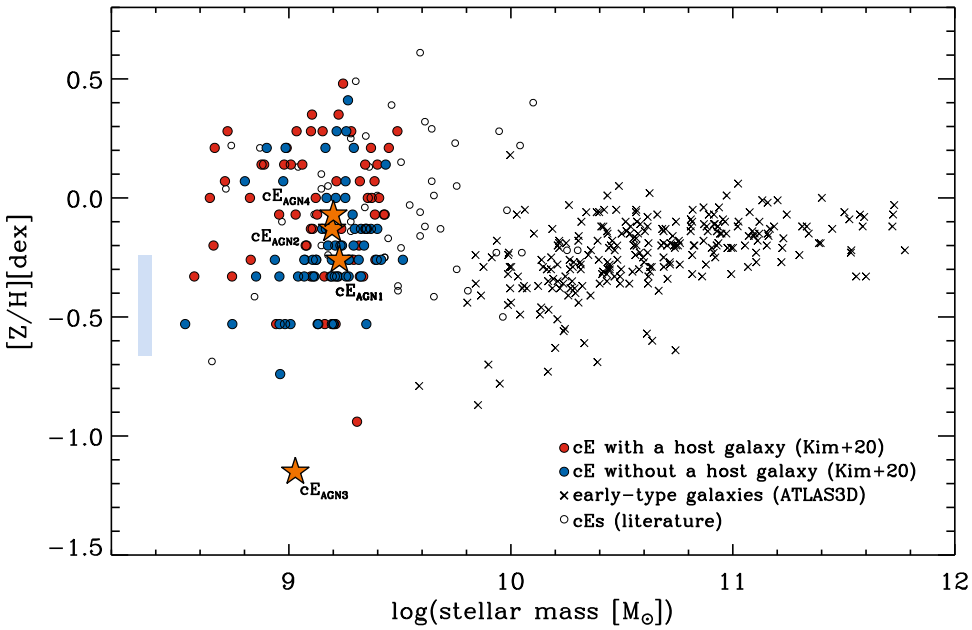


Figure 3. [Z/H] vs. stellar mass distribution for cEs. The four cE_{AGNs} are denoted by orange stars. The red and blue filled circles represent cEs with and without a bright host galaxy, respectively, from Kim et al. (2020). The open circles denote cEs compiled from the literature (Norris et al. 2014; Guérou et al. 2015; Janz et al. 2016; Ferré-Mateu et al. 2018, 2021a). The crosses are early-type galaxies from ATLAS3D (McDermid et al. 2015). The range of [Z/H] values (−0.24 to −0.66) of the cE_{AGNs} provided by Chilingarian et al. (2017) are denoted by the vertical bar.

should also reflect star formation activity. AGNs might be rare in cEs with old ages because these galaxies are devoid of gas for feeding central BHs. It has been shown that the majority of cEs typically have stellar populations with intermediate to old ages (>8 Gyr) and solar or oversolar metallicities (Ferré-Mateu et al. 2018, 2021a; Kim et al. 2020). However, a fraction of cEs also show relatively young ages (<5 Gyr) and sub-solar metallicities (see Figure 10 of Ferré-Mateu et al. 2021a, for a dichotomy in the age distribution). The mean ages of our cE_{AGNs} are 2−4 Gyr, which is indicative of star formation in recent epochs. In addition, SDSS emission line diagnostics have not identified ongoing star formation. Therefore, a plausible fuel for the triggering of AGN activity in cE_{AGNs} may be residual gas related to the star formation events that have recently ceased. This can provide a sustained supply of gas that could generate low-level AGN activity.

In their recent studies, Ferré-Mateu et al. (2018, 2021a) found that the majority of field cEs with no host galaxies exhibit slower and more extended star formation timescales than their counterparts in groups and clusters. Some isolated cEs show low star formation rates up to the present time. This type of star formation history (SFH) is typical of low-mass galaxies (e.g., Thomas et al. 2005), implying that isolated cEs are intrinsically low-mass cEs rather than objects formed from the stripping process of massive progenitors. The observed young ages and moderately low metallicities of our cE_{AGNs} reinforce the hypothesis of extended SFHs of isolated cEs, which is most likely responsible for the connection with their AGN activity.

It has been proposed that cEs are a mixture of galaxies with two possible origins. Different predictions for the properties of such cEs in different parameter spaces are expected. If cEs are the tidally stripped remnants of large, more massive progenitor galaxies, the properties of the core would likely be maintained, while a large fraction of the outer envelope would be removed. However, if cEs are intrinsic low-mass objects, they would retain their characteristics and follow the low-mass end of the local scaling relations described by massive early-type galaxies. In this respect, measuring the BH mass would provide another diagnostic tool for constraining the origin of cEs (see also Ferré-Mateu et al. 2021b). The BH masses of stripped cEs should correspond to those of massive progenitor galaxies. Thus, these cEs should deviate from the relation between BH mass and stellar mass because they have higher BH masses than galaxies with comparable stellar masses (e.g., two tidally stripped cEs, M32 and NGC 4486B, right panel of Figure 2; see also Figure 9 of Chilingarian et al. 2018). If cEs are bona fide low-mass classical early-type galaxies, they would conform to the BH mass–stellar mass relation. All four cE_{AGNs} in this study are in agreement with the observed relation between the BH masses and stellar velocity dispersions (and K-band luminosities) of their host galaxies. This is additional evidence that cE_{AGNs} in isolated environments are intrinsic low-mass early-type galaxies revealing BH properties commensurate with their stellar masses. Accordingly, we suggest that the BH properties of cEs are one of the key parameters responsible for distinguishing between the two different cE formation processes. In combination with the results reported in this Letter, by measuring BH masses for a large sample of cEs with massive nearby host galaxies, their tidally stripped origin could be further confirmed in future works.

We are grateful to the anonymous referee for helpful comments and suggestions that improved the clarity and quality of this Letter. We thank Hyunjin Jeong for providing the errors of age and [Z/H] of cEs. S.C.R. and K.O. contributed equally to this work as corresponding authors. This work was supported by the National Research Foundation of Korea through grants 2018R1A2B2006445 (S.C.R.), 2020R1C1C1005462 (K.O.), and 2019R1I1A1A01061237 (S.K.).

ORCID iDs

Soo-Chang Rey https://orcid.org/0000-0002-0041-6490
Kyuseok Oh https://orcid.org/0000-0002-5037-951X
Suk Kim https://orcid.org/0000-0003-3474-9047

References

Aird, J., Coil, A. L., & Georgakakis, A. 2019, MNRAS, 484, 4360
Baldwin, J. A., Phillips, M. M., & Terlevich, R. 1981, PASP, 93, 5
Baron, D., & Ménard, B. 2019, MNRAS, 487, 3404
Bekki, K., Couch, W. J., Drinkwater, M. J., & Gregg, M. D. 2001, ApJ, 557, L39
Bertin, E., & Arnouts, S. 1996, A&AS, 117, 393
Bruzual, G., & Charlot, S. 2003, MNRAS, 344, 1000
Cappellari, M., & Emsellem, E. 2004, PASP, 116, 138
Chilingarian, I., Cayatte, V., Revaz, Y., et al. 2009, Sci, 326, 1379
Chilingarian, I., & Zolotukhin, I. 2015, Sci, 348, 418
Chilingarian, I. V., Katkov, I. Y., Zolotukhin, I. Y., et al. 2018, ApJ, 863, 1
Chilingarian, I. V., Zolotukhin, I. Y., Katkov, I. Y., et al. 2017, ApJS, 228, 14
Dey, A., Schlegel, D. J., Lang, D., et al. 2019, AJ, 157, 168
Du, M., Debattista, V. P., Ho, L. C., et al. 2019, ApJ, 875, 58
Ferré-Mateu, A., Durre, M., Forbes, D. A., et al. 2021a, MNRAS, 503, 5455
Ferré-Mateu, A., Forbes, D. A., Romanowsky, A. J., Janz, J., & Dixon, C. 2018, MNRAS, 473, 1819
Ferré-Mateu, A., Mezcua, M., & Barrows, R. S. 2021b, MNRAS, 506, 4702
Guérou, A., Emsellem, E., McDermid, R. M., et al. 2015, ApJ, 804, 70
Gültekin, K., Richstone, D. O., Gebhardt, K., et al. 2009, ApJ, 698, 198
Huxor, A. P., Phillipps, S., & Price, J. 2013, MNRAS, 430, 1956
Huxor, A. P., Phillipps, S., Price, J., & Harniman, R. 2011, MNRAS, 414, 3557
Janz, J., Norris, M. A., Forbes, D. A., et al. 2016, MNRAS, 456, 617
Kauffmann, G., Heckman, T. M., Tremonti, C., et al. 2003, MNRAS, 346, 1055
Kewley, L. J., Dopita, M. A., Sutherland, R. S., Heisler, C. A., & Trevena, J. 2001, ApJ, 556, 121
Kewley, L. J., Groves, B., Kauffmann, G., & Heckman, T. 2006, MNRAS, 372, 961
Kim, S., Jeong, H., Rey, S.-C., et al. 2020, ApJ, 903, 65
Kormendy, J., & Bender, R. 2012, ApJS, 198, 2
Kormendy, J., Bender, R., Magorrian, J., et al. 1997, ApJL, 482, L139
Kormendy, J., Fisher, D. B., Cornell, M. E., & Bender, R. 2009, ApJS, 182, 216
Kormendy, J., & Ho, L. C. 2013, ARA&A, 51, 511
Man, Z.-y., Peng, Y.-j., Kong, X., et al. 2019, MNRAS, 488, 89
Martinović, N., & Micic, M. 2017, MNRAS, 470, 4015
McDermid, R. M., Alatalo, K., Blitz, L., et al. 2015, MNRAS, 448, 3484
Mieske, S., Frank, M. J., Baumgardt, H., et al. 2013, A&A, 558, A14
Norris, M. A., Kannappan, S. J., Forbes, D. A., et al. 2014, MNRAS, 443, 1151
Oh, K., Sarzi, M., Schawinski, K., & Yi, S. K. 2011, ApJS, 195, 13
Oh, K., Yi, S. K., Schawinski, K., et al. 2015, ApJS, 219, 1
Paudel, S., Hilker, M., Ree, C. H., & Kim, M. 2016, ApJL, 820, L19
Paudel, S., Lisker, T., Hansson, K. S. A., & Huxor, A. P. 2014, MNRAS, 443, 446
Paudel, S., & Ree, C. H. 2014, ApJL, 796, L14
Sales, L. V., Navarro, J. F., Abadi, M. G., & Steinmetz, M. 2007, MNRAS, 379, 1475
Sánchez-Blázquez, P., Peletier, R. F., Jiménez-Vicente, J., et al. 2006, MNRAS, 371, 703
Sarzi, M., Falcón-Barroso, J., Davies, R. L., et al. 2006, MNRAS, 366, 1151
Saulder, C., van Kampen, E., Chilingarian, I. V., Mieske, S., & Zeilinger, W. W. 2016, A&A, 596, A14
Schawinski, K., Thomas, D., Sarzi, M., et al. 2007, MNRAS, 382, 1415
Schlafly, E. F., & Finkbeiner, D. P. 2011, ApJ, 737, 103
Tempel, E., Tamm, A., Gramann, M., et al. 2014, A&A, 566, A1
Thomas, D., Maraston, C., Bender, R., & Mendes de Oliveira, C. 2005, ApJ, 621, 673
Urrutia Zapata, F., Fellhauer, M., Alarcón Jara, A. G., Matus Carrillo, D. R., & Aravena, C. A. 2019, MNRAS, 489, 2746
van der Marel, R. P., Sigurdsson, S., & Hernquist, L. 1997, ApJ, 487, 153
Wirth, A., & Gallagher, J. S., III 1984, ApJ, 282, 85
Xiao, T., Barth, A. J., Greene, J. E., et al. 2011, ApJ, 739, 28